A Truly Two-Dimensional Discretization of Drift-Diffusion Equations on Cartesian Grids

Roberta Bianchini, Laurent Gosse

A Truly Two-Dimensional Discretization of Drift-Diffusion Equations on Cartesian Grids

Article *in* SIAM Journal on Numerical Analysis · September 2017

DOI: 10.1137/17M1151353

2 authors:


Roberta Bianchini
Ecole normale supérieure de Lyon


Laurent Gosse
Italian National Research Council

A TRULY TWO-DIMENSIONAL DISCRETIZATION OF DRIFT-DIFFUSION EQUATIONS ON CARTESIAN GRIDS

ROBERTA BIANCHINI* AND LAURENT GOSSE†

Abstract. A genuinely two-dimensional discretization of general drift-diffusion (including incompressible Navier-Stokes) equations is proposed. Its numerical fluxes are derived by computing the radial derivatives of "bubbles" which are deduced from available discrete data by exploiting the stationary Dirichlet-Green function of the convection-diffusion operator. These fluxes are reminiscent of Scharfetter-Gummel's in the sense that they contain modified Bessel functions which allow to pass smoothly from diffusive to drift-dominating regimes. For certain flows, monotonicity properties are established in the vanishing viscosity limit ("asymptotic monotony") along with second-order accuracy when the grid is refined. Practical benchmarks are displayed to assess the feasibility of the scheme, including the "western currents" with a Navier-Stokes-Coriolis model of ocean circulation.

Key words. Bubbles; Drift-Diffusion; Green-Dirichlet function; Navier-Stokes-Coriolis.

AMS subject classifications. 65M06, 65N80, 76D05, 76U05, 86A05.

1. Introduction.

The general scope of the present article is to address a "genuinely two-dimensional" numerical analysis, involving mostly finite-differences, of general (possibly weakly-nonlinear, i.e. mean-field), drift-diffusion equation,

$$\partial_t \rho(t,x,y) - \nabla\cdot(\varepsilon\,\nabla\rho - \rho\nabla\Phi) = 0 \quad \text{in} \quad \Omega\subset\mathbb{R}^2, \qquad \varepsilon>0, \tag{1.1}$$

where Ω is, most often, the square domain $(0,1)^2$ and $\partial\Omega$ its boundary. Convenient boundary conditions supplement (1.1), like e.g., Dirichlet or Neumann. The potential Φ can be prescribed or self-consistently related to $\rho(t,x,y)$ through a strictly elliptic, attractive or repulsive (Coulomb or gravitational interactions), equation,

$$-\Delta\Phi + \lambda\Phi = \pm\rho, \qquad \lambda \geq 0, \quad \text{in} \quad \Omega\subset\mathbb{R}^2, \tag{1.2}$$

to which are added boundary conditions as well. An elementary calculation shows that (1.1)–(1.2) encompasses the 2D incompressible Navier-Stokes equations, too,

$$\partial_t \omega(t,x,y) - \nabla\cdot\left(\frac{\nabla\omega}{Re} - \omega\,\nabla^\perp\psi\right) = 0, \qquad -\Delta\psi = \omega. \tag{1.3}$$

The stream function ψ is related to the vorticity $\omega = \nabla^\perp\cdot\vec{U}$, where $\vec{U}=(u,v)$ stands for the fluid's velocity and $0 < Re$, for the Reynolds number.

1.1. Numerical fluxes as radial derivatives of "Green bubbles".

Many numerical schemes for either (1.1) or (1.3) proceed by discretizing the continuity equations in both horizontal and vertical directions (dimensional splitting) in such a manner that discrete drift and diffusion terms don't see each other. This is a different situation from the simpler, one-dimensional, case where the "uniformly accurate" (or

*DIPARTIMENTO DI MATEMATICA, UNIVERSITÀ DEGLI STUDI DI ROMA "TOR VERGATA", VIA DELLA RICERCA SCIENTIFICA 1, I-00133 ROME (ITALY), IAC–CNR "MAURO PICONE" (SEZIONE DI ROMA), VIA DEI TAURINI 19, 00185 ROME (ITALY) BIANCHIN@MAT.UNIROMA2.IT

†IAC–CNR "MAURO PICONE" (SEZIONE DI ROMA), VIA DEI TAURINI 19, 00185 ROME (ITALY) L.GOSSE@BA.IAC.CNR.IT

"asymptotic-preserving", AP) Il'in/Scharfetter-Gummel algorithm [21, 25, 31] allows to treat the 1D drift-diffusion operator as a whole. Consider, for $\epsilon > 0$,

$$\partial_t \rho(t,x) + \partial_x J(t,x) = 0, \qquad J := -\epsilon\, \partial_x \rho + \rho.$$

Denote $\rho_j^n = \rho(t^n, x_j = j\Delta x)$, a reliable (constant) numerical flux $J^n_{j-\frac{1}{2}}$ can be derived at each interface of the grid so that, one gets a forward time-marching scheme,

$$\frac{\rho_j^{n+1} - \rho_j^n}{\Delta t} + \frac{J^n_{j+\frac{1}{2}} - J^n_{j-\frac{1}{2}}}{\Delta x} = 0. \tag{1.4}$$

Clearly, $J^n_{j-\frac{1}{2}}$ is the flux related to the $\mathcal{L}$-spline interpolation [32] at time t^n, that is, the piecewise steady-state curve linking each (x_{j-1}, ρ^n_{j-1}) to its neighbor (x_j, ρ_j^n),

$$-\epsilon \exp(x/\epsilon) \frac{d}{dx}\Big(\exp(-x/\epsilon) \bar\rho(x) \Big) = J^n_{j-\frac{1}{2}}, \quad x \in (x_{j-1}, x_j). \tag{1.5}$$

and it allows (1.4) to be reliable whatever the "Peclet number" $\Delta x/2\epsilon$. Hence, a chal-

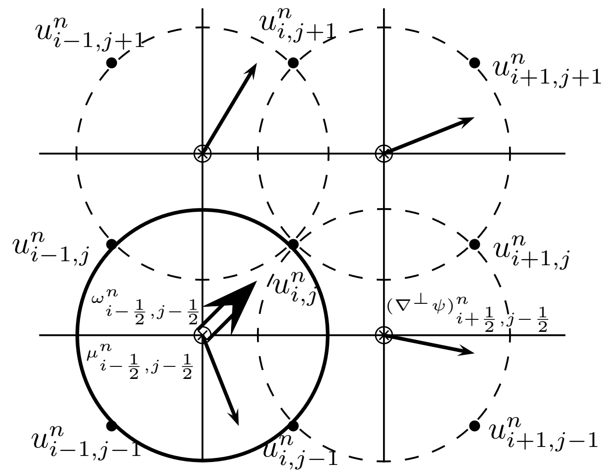

FIGURE 1.1. *Radial derivative "⇒" with Delaunay circles on a uniform Cartesian grid.*

lenging question [2] is to extend such a construction to multi-dimensional problems, for which the simplest continuity equation reads $\partial_t \rho + \nabla \cdot \mathbf{J} = 0$, $\mathbf{J} = \epsilon \nabla \rho - \rho$. Its steady-state, $\nabla \cdot \mathbf{J} = 0$, doesn't allow to easily deduce a distinguished flux function, even on a uniform Cartesian computational grid. Hereafter, a complete resolution of that question is given, in the form of a 2D finite-difference scheme for (1.1), build again by considering a piecewise-steady "bubble interpolation" of discrete data.

- Denoting x_i, y_j a generic grid point in the computational domain, Delaunay-type disks are drawn around each of the 4 neighboring nodes $x_{i\pm\frac{1}{2}}, y_{j\pm\frac{1}{2}}$. Inside each disk, a (local) steady-state solution is derived by means of the Dirichlet-Green function (2.18) of the convection-diffusion operator (2.1).
- Radial derivatives at the center of each disk (at each node) are computed by means of an exact formula (2.19) involving modified Bessel functions I_n. Our 2D fluxes are defined as their approximation resulting from the trigonometric interpolation of the 4 values available on each circle: see (3.5) and (3.7).

- Time-marching schemes can be deduced, see e.g. (4.2) and (4.4), for which various monotony and accuracy properties are established. In practice, they were set up mostly on Navier-Stokes equations (1.3), possibly in presence of a Coriolis force modeled by means of a "β-plane approximation".

Our piecewise-steady interpolation is somewhat reminiscent of "bubbles" [5, 7]; here, neither differential operators nor spatial directions are split in our calculations so that the exponential functions, typical of 1D problems endowed with sharp layers, leave the stage to a sequence of modified Bessel functions, I_n, in 2D. It traces back to "discrete weighted mean" agorithms [15], nowadays rephrased as "tailored methods" [19].

1.2. Plan of the paper. Fig. 1.1 appears to be similar to Fig. 2 in [18, page 176]; however, the fluxes we intend to derive here are evaluated at each disk's center, thus are different from these former ones, which are computed on each disk's boundary. Section 2 contains most of the analytical calculations which are necessary to derive the Dirichlet-Green (sometimes called "companion") function for convection-diffusion (2.1). We perform a symmetrization of the skew-adjoint transport operator thanks to an exponential modulation (2.3) in order to retrieve an Helmholtz-type equation (2.2). Then, in Section 2.3, the corresponding Green function with homogeneous boundary condition is found, along with its radial derivative in Section 2.4: consistency with the well-known Poisson potential is checked. Section 3 contains the practical computation of numerical fluxes: after the trigonometric interpolation in Section 3.1, radial derivatives are displayed in Section 3.2. Specific properties of the resulting scheme are studied in Section 4, where a notion of "asymptotic monotony" (see Def. 1) is defined in the limit of vanishing viscosity: our main results are stated in Theorem 1. Numerical tests are presented in Section 5, mostly on incompressible Navier-Stokes equations, possibly in presence of a Coriolis term and an external forcing rendering the wind in ocean circulation models, see [9] and Fig. 5.5. Some tests were also performed on the classical lid-driven cavity problem, see Fig. 5.3 and [16].

2. A formalism based on Green-Dirichlet functions. Let $R > 0$ and D stands for the (open) disk with radius $R > 0$, centered in $\vec{0}$. Here C is the circle of identical radius, so that $C = \partial \bar{D}$. As mentioned before, here we solve an homogeneous boundary-value problem endowed with inhomogeneous boundary data,

$$\mathcal{L}_\varepsilon[u] = -\varepsilon \Delta u + \mathbf{V} \cdot \nabla u = 0 \text{ in } D, \qquad u(x,y) = h(x,y) \text{ on } C, \tag{2.1}$$

where $\mathbf{V} = (V_1, V_2) \in \mathbb{R}^2$ is a constant vector and "$\cdot$" stands for the $\mathbb{R}^2$ scalar product. It is customary to symmetrize $\mathcal{L}_\varepsilon$ by means of an associated Klein-Gordon (or modified Helmholtz) operator, hereafter denoted by $\mathcal{H}_\varepsilon$:

$$\mathcal{H}_\varepsilon[v] = -\Delta v + \left|\frac{\mathbf{V}}{2\varepsilon}\right|^2 v(x,y) = 0, \qquad \omega_\varepsilon := \left|\frac{\mathbf{V}}{2\varepsilon}\right|, \tag{2.2}$$

with $|\cdot|$ standing for the Euclidean norm in $\mathbb{R}^2$. It is well-known that, if $u(x,y)$ solves $\mathcal{L}_\varepsilon[u]$ in $\mathbb{R}^2$, then its "exponential modulation",

$$v(x,y) = \exp\left(-\frac{\mathbf{V}}{2\varepsilon} \cdot (x,y)\right) u(x,y), \text{ solves } \mathcal{H}_\varepsilon[v] = 0. \tag{2.3}$$

So, G^0_ε, the Green-Dirichlet function of $\mathcal{L}_\varepsilon$ vanishing on C, comes from the one of $\mathcal{H}_\varepsilon$.

2.1. Green's formalism for $\mathcal{L}_\varepsilon$. Let $\mathcal{L}_\varepsilon^*$ stand for the adjoint of $\mathcal{L}_\varepsilon$ and u be a solution to (2.1), namely $\mathcal{L}_\varepsilon[u] = 0$. Green's identity (see [11]) yields:

$$\int_D u^*\,\mathcal{L}_\varepsilon[u] - u\,\mathcal{L}_\varepsilon^*[u^*]\,\mathrm{d}x\,\mathrm{d}y = \int_C u(q^*\cdot\vec{n}) - u^*(q\cdot\vec{n})\,\mathrm{d}\sigma(x,y), \tag{2.4}$$

where

$$q = \varepsilon\nabla u - \frac{\mathbf{V}}{2}u, \qquad q^* = \varepsilon\nabla u^* + \frac{\mathbf{V}}{2}u^*$$

are fluxes associated to u, u^*. Let $u_P^*(Q) = g_\varepsilon^0(Q,P)$ be the Dirichlet-Green function of the adjoint operator acting on the $Q = (x,y)$ variable, with $P = (\xi,\zeta)$ fixed, then

$$\mathcal{L}_\varepsilon^*[u_P^*] = \mathcal{L}_\varepsilon^*[g_\varepsilon^0(Q,P)] = \delta(Q-P), \qquad u_P^*(Q) = 0 \text{ for } Q\in C,$$

where, in standard notation, P, Q are source/receiver points in D. Substituting u_P^* and u, i.e. the solution to the original problem (2.1), in (2.4),

$$-\int_D u(Q)\delta(Q-P)\,\mathrm{d}Q = -u(P) = \varepsilon\int_C h(Q)\frac{\partial u_P^*(Q)}{\partial\vec{n}_Q}\,\mathrm{d}Q. \tag{2.5}$$

Considering again the Green identity in (2.4) and setting $u = G_\varepsilon^0(Q,S)$ be the Green-Dirichlet function of $\mathcal{L}_\varepsilon$ acting on Q, where S is a fixed point, we symbolically write

$$\mathcal{L}_\varepsilon[G_\varepsilon^0(Q,S)] = \delta(Q-S), \qquad G_\varepsilon^0(Q,S) = 0 \quad \text{for } Q\in C,$$

Inserting u and $u^* = u_P^*$ so defined in (2.4), this gives

$$\int_D g_\varepsilon^0(Q,P)\delta(Q-S) - G_\varepsilon^0(Q,S)\delta(Q-P)\,\mathrm{d}Q = 0,$$

which yields, for any choice of $P, R\in D$,

$$g_\varepsilon^0(S,P) = G_\varepsilon^0(P,S), \tag{2.6}$$

where

$$g_\varepsilon^0(S,P) = u_P^*(S). \tag{2.7}$$

Identity (2.6) means that the Green-Dirichlet function $g_\varepsilon^0(P,Q)$ of the adjoint operator $\mathcal{L}_\varepsilon^*$, with Dirac mass centered in P, is obtained just by switching the points coordinates of the corresponding Green-Dirichlet function $G_\varepsilon^0(P,Q)$ associated to $\mathcal{L}_\varepsilon$. Because of the skew-symmetry of the convection part, $\mathcal{L}_\varepsilon$ is not self-adjoint, so the Green-Dirichlet function G_ε^0 is not symmetric, depending on the sing of the vector $P-Q$. Now, let us go back to the expression for $u(P)$ in (2.5), namely

$$u(P) = -\varepsilon\int_C h(Q)\frac{\partial u_P^*(Q)}{\partial\vec{n}_Q}\,\mathrm{d}Q = -\varepsilon\int_C h(Q)(\nabla u_P^*(Q)\cdot\vec{n})\,\mathrm{d}Q.$$

Since $u_P^*(Q) = g_\varepsilon^0(Q,P)$, equality (2.7) yields

$$u(P) = -\varepsilon\int_C h(Q)(\nabla g_\varepsilon^0(Q,P)\cdot\vec{n})\,\mathrm{d}Q.$$

By using the previous identity in (2.6), this amounts to,

$$u(P) = -\varepsilon \int_C h(Q)(\nabla G_\varepsilon^0(P,Q)\cdot \vec{n})\,\mathrm{d}Q.$$

Introducing the radial coordinates as follows:

$$P = (r,\theta), \qquad Q = (\rho,\psi),$$

we get the "double-layer potential" expression of u,

$$\boxed{u(r,\theta) = -\varepsilon \int_0^{2\pi} h(\psi)\frac{\partial G_\varepsilon^0}{\partial \rho}(r,\theta;\rho=R,\psi)\,R\,\mathrm{d}\psi.} \tag{2.8}$$

The radial derivative of the solution u will be of crucial importance: it reads,

$$\boxed{\frac{\partial u}{\partial r}(r=0,\theta) = -\varepsilon \int_0^{2\pi} h(\psi)\frac{\partial^2 G_\varepsilon^0}{\partial r \partial \rho}(r=0,\theta;\rho=R,\psi)\,R\,\mathrm{d}\psi.} \tag{2.9}$$

A suitable assemblage of the radial derivative in (2.9), with respect to the four disks of the stencil, provides the numerical flux at each node of the computational grid.

2.2. Fundamental solution of $\mathcal{L}_\varepsilon$ in full space. Here we consider the full space Green function G_ε – or fundamental solution – associated to the operator $\mathcal{L}_\varepsilon$. According with the Green formalism,

$$\mathcal{L}_\varepsilon[G_\varepsilon] = \delta(P-Q), \qquad P,Q\in\mathbb{R}^2.$$

Taking a constant vector $\mathbf{V}\in\mathbb{R}^2$, according to (2.3), following [11] we can write

$$G_\varepsilon(P,Q) = \exp\left(\frac{\mathbf{V}\cdot(P-Q)}{2\varepsilon}\right)H_\varepsilon(P,Q), \tag{2.10}$$

such that H_ε is the fundamental solution of $\mathcal{H}_\varepsilon$ defined in (2.2).

$$-\Delta H_\varepsilon + \left|\frac{\mathbf{V}}{2\varepsilon}\right|^2 H_\varepsilon = \frac{1}{\varepsilon}\exp\left(-\frac{\mathbf{V}\cdot(P-Q)}{2\varepsilon}\right)\delta(P-Q).$$

Thus, it is straightforward to see that

$$\delta(P-Q) = \mathcal{L}_\varepsilon(G_\varepsilon) = \exp\left(\frac{\mathbf{V}\cdot(P-Q)}{2\varepsilon}\right)\left(-\varepsilon\Delta H_\varepsilon + \left|\frac{\mathbf{V}}{2\sqrt{\varepsilon}}\right|^2 H_\varepsilon\right),$$

so that (2.10) is the desired full-space Green function of $\mathcal{L}_\varepsilon$.

2.3. Green-Dirichlet function for $\mathcal{H}_\varepsilon$ in a disk. Taking advantage of (2.10), we are now interested in deriving the Dirichlet-Green function in a disk, $G_\varepsilon^0(P,Q)$. for $\mathcal{L}_\varepsilon$, acting on the variable Q and centered in P:

$$\begin{cases} \mathcal{L}_\varepsilon[G_\varepsilon^0] &= \delta(P-Q),\\ G_\varepsilon^0(P,Q) &= 0 \text{ for } Q\in C,\\ G_\varepsilon^0(P,Q) &= \exp\left(\frac{\mathbf{V}\cdot(P-Q)}{2\varepsilon}\right)H_\varepsilon^0(P,Q), \end{cases} \tag{2.11}$$

being $H^0_\varepsilon(P,Q)$ the Dirichlet-Green function associated with $\mathcal{H}_\varepsilon$ in (2.2) and

$$\omega_\varepsilon = \left|\frac{\mathbf{V}}{2\varepsilon}\right|, \qquad \frac{\mathbf{V}}{2\varepsilon} = \omega_\varepsilon(\cos\mu, \sin\mu) \text{ for any } \mu \in (-\pi,\pi), \tag{2.12}$$

along with,

$$\begin{aligned}\frac{\mathbf{V}\cdot(P-Q)}{2\varepsilon} &= \omega_\varepsilon\big((r\cos\theta - \rho\cos\psi)\cos\mu + (r\sin\theta - \rho\sin\psi)\sin\mu\big)\\ &= \omega_\varepsilon\big(r\cos(\theta-\mu) - \rho\cos(\psi-\mu)\big).\end{aligned}$$

PROPOSITION 1. *Let D be the disk centered at the origin with radius $R>0$, then the Green function associated with the "modified Helmholtz" operator $\mathcal{H}_\varepsilon$ in (2.2) with Dirichlet boundary condition is,*

$$H^0_\varepsilon(r,\theta;\rho,\psi) = \frac{1}{2\pi}\sum_{n\in\mathbb{Z}} \frac{I_{|n|}(\omega_\varepsilon r_<)}{I_{|n|}(\omega_\varepsilon R)}\left(I_{|n|}(\omega_\varepsilon R)K_{|n|}(\omega_\varepsilon r_>) - I_{|n|}(\omega_\varepsilon r_>)K_{|n|}(\omega_\varepsilon R)\right). \tag{2.13}$$

where $r_< := \min\{r,\rho\}$, $r_< := \max\{r,\rho\}$, and I_n, K_n are modified Bessel functions.

Proof. It is convenient to switch to radial coordinates: the Green function for the "modified Helmholtz equation" (2.2) solves,

$$\frac{1}{r}\frac{\partial}{\partial r}\left(r\frac{\partial H^0_\varepsilon}{\partial r}\right) + \frac{1}{r^2}\frac{\partial^2 H^0_\varepsilon}{\partial\theta^2} - \omega_\varepsilon^2 H^0_\varepsilon = -\frac{\delta(r-\rho)\delta(\theta-\psi)}{r}, \tag{2.14}$$

where $0 < r,\rho < R$, $0 \le \theta,\psi \le 2\pi$, with boundary condition $H^0_\varepsilon(R,\theta;\rho,\psi) = 0$. Clearly, (2.14) rewrites as an Helmholtz equation where ω_ε is replaced by $i\omega_\varepsilon$,

$$\frac{1}{r}\frac{\partial}{\partial r}\left(r\frac{\partial H^0_\varepsilon}{\partial r}\right) + \frac{1}{r^2}\frac{\partial^2 H^0_\varepsilon}{\partial\theta^2} + (i\omega_\varepsilon)^2 H^0_\varepsilon = -\frac{\delta(r-\rho)\delta(\theta-\psi)}{r}. \tag{2.15}$$

Yet, we provide an expression of the Dirichlet-Green function for Helmholtz equation with frequency $\lambda = i\omega_\varepsilon$. First of all, by using the Fourier basis, it comes

$$\delta(\theta-\psi) = \frac{1}{2\pi} + \frac{1}{\pi}\sum_{n=1}^{\infty}\cos(n(\theta-\psi)) = \frac{1}{2\pi}\sum_{n=-\infty}^{\infty}\cos(n(\theta-\psi)),$$

which implies that the solution to (2.15) presents the following form:

$$H^0_\varepsilon(r,\theta;\rho,\psi) = \sum_{n=-\infty}^{\infty} h^0_n(r,\rho)\,\cos(n(\theta-\psi)).$$

It is well-known that a particular solution to equation (2.15) is given by

$$-\frac{1}{4}Y_0(i\omega_\varepsilon\sqrt{r^2+\rho^2-2r\rho\cos(\theta-\psi)}),$$

where Y_0 is the zero order Bessel function of the second kind. The general solution to (2.14) can be expressed by means of J_n, the Bessel functions of the first kind,

$$H^0_\varepsilon(r,\theta;\rho,\psi) = -\frac{1}{4}Y_0(i\omega_\varepsilon\sqrt{r^2+\rho^2-2r\rho\cos(\theta-\psi)}) + \sum_{n=-\infty}^{\infty} A_n J_n(i\omega_\varepsilon r)\cos(n(\theta-\psi)).$$

Homogeneous boundary conditions for H^0_ε read $H^0_\varepsilon(R,\theta;\rho,\psi)=0$ bring

$$\frac{1}{4}Y_0(i\omega_\varepsilon\sqrt{R^2+\rho^2-2R\rho\cos(\theta-\psi)})=\sum_{n=-\infty}^{\infty}A_nJ_n(i\omega_\varepsilon R)\cos(n(\theta-\psi)),$$

and, from the addition theorem for Bessel function, see [11],

$$Y_0(i\omega_\varepsilon\sqrt{r^2+\rho^2-2r\rho\cos(\theta-\psi)})=\sum_{n=-\infty}^{\infty}J_n(i\omega_\varepsilon\rho)J_n(i\omega_\varepsilon r)\cos(n(\theta-\psi)).$$

Accordingly,

$$\frac{1}{4}\sum_{n=-\infty}^{\infty}J_n(i\omega_\varepsilon\rho)Y_n(i\omega_\varepsilon R)\cos(n(\theta-\psi))=\sum_{n=-\infty}^{\infty}A_nJ_n(i\omega_\varepsilon R)\cos(n(\theta-\psi)),$$

so that,

$$\boxed{\forall n\in\mathbb{Z},\qquad A_n=\frac{J_n(i\omega_\varepsilon\rho)Y_n(i\omega_\varepsilon R)}{4J_n(i\omega_\varepsilon R)}.}$$

This gives the following expression:

$$\begin{aligned}H^0_\varepsilon(r,\theta;\rho,\psi)=&-\frac{1}{4}Y_0(i\omega_\varepsilon\sqrt{r^2+\rho^2-2r\rho\cos(\theta-\psi)})\\&+\sum_{n=-\infty}^{\infty}\frac{Y_n(i\omega_\varepsilon R)}{4J_n(i\omega_\varepsilon R)}J_n(i\omega_\varepsilon\rho)J_n(i\omega_\varepsilon r)\cos(n(\theta-\psi)).\end{aligned}\tag{2.16}$$

By using again the addition theorem in (2.16) and following [11], one gets the Dirichlet-Green function for the Helmholtz equation in (2.15),

$$H^0_\varepsilon(r,\theta;\rho,\psi)=-\frac{1}{4}\sum_{n\in\mathbb{Z}}\frac{J_n(i\omega_\varepsilon r_<)}{J_n(i\omega_\varepsilon R)}\Big(J_n(i\omega_\varepsilon R)Y_n(i\omega_\varepsilon r_>)-Y_n(i\omega_\varepsilon R)J_n(i\omega_\varepsilon r_>)\Big)\cos(n(\theta-\psi)),\tag{2.17}$$

First and second kind Bessel functions with imaginary arguments reduce to,

$$J_n(ix)=e^{n\pi i/2}I_n(x),\qquad Y_n(ix)=e^{(n+1)\pi i/2}I_n(x)-\frac{2}{\pi}e^{-n\pi i/2}K_n(x),$$

so that (2.17) rewrites in terms of the modified Bessel functions of the first and second kind, bringing the expression (2.13), as stated in the Proposition. □

Following [11], the expression of G^0_ε is immediately deduced from the one of H^0_ε.

Corollary 1. *With the notation of Proposition 1, and $H^0_\varepsilon(r,\theta;\rho,\psi)$ being given in (2.13), the Dirichlet-Green function for convection-diffusion (2.1) in D is,*

$$G^0_\varepsilon(r,\theta;\rho,\psi)=\exp\left(\frac{\mathbf{V}\cdot(P-Q)}{2\varepsilon}\right)H^0_\varepsilon(r,\theta;\rho,\psi).\tag{2.18}$$

2.4. Radial derivatives of $G^0_\varepsilon(r,\theta;\rho,\psi)$. Following Proposition 1, it holds:
PROPOSITION 2. *Let $\theta \in (-\pi,\pi)$ be a direction, and denote*

$$E(\psi) = \exp(-\omega_\varepsilon R\cos(\psi-\mu)),$$

then, the radial derivative (2.9) reads,

$$\begin{aligned}\frac{\partial u}{\partial r}(r=0,\theta) \quad = \quad & \frac{\varepsilon\omega_\varepsilon}{2\pi}\left(\frac{\cos(\theta-\mu)}{I_0(\omega_\varepsilon R)}\int_0^{2\pi} h(\psi)E(\psi)\,\mathrm{d}\psi\right. \\ & \left.+\frac{1}{I_1(\omega_\varepsilon R)}\int_0^{2\pi} h(\psi)E(\psi)\cos(\theta-\psi)\,\mathrm{d}\psi\right).\end{aligned} \tag{2.19}$$

Proof. Denoting by χ_E the indicator function of a set E, let

$$r_< := \min\{r,\rho\} = r\chi_{\{r-\rho<0\}} + \rho\chi_{\{r-\rho>0\}}, \qquad \frac{\partial \min\{r,\rho\}}{\partial\rho} = \chi_{\{r-\rho>0\}},$$
$$r_> := \max\{r,\rho\} = \rho\chi_{\{r-\rho<0\}} + r\chi_{\{r-\rho>0\}}, \qquad \frac{\partial \max\{r,\rho\}}{\partial\rho} = \chi_{\{r-\rho<0\}}.$$

This provides the following expression for the partial derivative in ρ of $H^0_\varepsilon(r,\theta;\rho,\psi)$,

$$\begin{aligned}\frac{\partial H^0_\varepsilon(r,\theta;\rho,\psi)}{\partial\rho} = \frac{\omega_\varepsilon}{2\pi}\sum_{n\in\mathbb{Z}}\Bigg\{ & \frac{I'_{|n|}(\omega_\varepsilon r_<)\chi_{\{r-\rho>0\}}}{I_{|n|}(\omega_\varepsilon R)}\Big(I_{|n|}(\omega_\varepsilon R)K_{|n|}(\omega_\varepsilon r_>) - I_{|n|}(\omega_\varepsilon r_>)K_{|n|}(\omega_\varepsilon R)\Big) \\ & +\frac{I_{|n|}(\omega_\varepsilon r_<)}{I_{|n|}(\omega_\varepsilon R)}\chi_{\{\rho-r>0\}}\Big(I_{|n|}(\omega_\varepsilon R)K'_{|n|}(\omega_\varepsilon r_>) - I'_{|n|}(\omega_\varepsilon r_>)K_{|n|}(\omega_\varepsilon R)\Big)\Bigg\}\cos(n(\theta-\psi)).\end{aligned} \tag{2.20}$$

In (2.8), it is meant to be $\rho = R$: hence, using the Wronskian relation [1, 15],

$$K_{|n|}(\omega_\varepsilon R)I'_{|n|}(\omega_\varepsilon R) - K'_{|n|}(\omega_\varepsilon R)I_{|n|}(\omega_\varepsilon R) = \frac{1}{\omega_\varepsilon R}, \tag{2.21}$$

one gets

$$\frac{\partial H^0_\varepsilon}{\partial\rho}(r,\theta;R,\psi) = \frac{1}{2\pi R}\sum_{n\in\mathbb{Z}}\frac{I_{|n|}(\omega_\varepsilon r)}{I_{|n|}(\omega_\varepsilon R)}\cos n(\psi-\theta),$$

and so

$$\frac{\partial H^0_\varepsilon}{\partial\rho}(0,\theta;R,\psi) = -\frac{1}{2\pi R I_0(\omega_\varepsilon R)}.$$

The radial derivative (2.9) also needs the expression of a "mixed derivative" of H^0_ε at $r=0, \rho=R$. From (2.20), and since $\chi_{\{\rho-r>0\}}\chi_{\{\rho-r<0\}} = 0$,

$$\begin{aligned}\frac{\partial^2 H^0_\varepsilon(r,\theta;\rho,\psi)}{\partial r\partial\rho} = \frac{\omega_\varepsilon}{2\pi}\sum_{n\in\mathbb{Z}}\Bigg\{ & \frac{I'_{|n|}(\omega_\varepsilon r_<)\delta(r-\rho)}{I_{|n|}(\omega_\varepsilon R)}\Big(I_{|n|}(\omega_\varepsilon R)K_{|n|}(\omega_\varepsilon r_>) - I_{|n|}(\omega_\varepsilon r_>)K_{|n|}(\omega_\varepsilon R)\Big) \\ & +\omega_\varepsilon\frac{I'_{|n|}(\omega_\varepsilon r_<)}{I_{|n|}(\omega_\varepsilon R)}\Big(I_{|n|}(\omega_\varepsilon R)K'_{|n|}(\omega_\varepsilon r_>) - I'_{|n|}(\omega_\varepsilon r_>)K_{|n|}(\omega_\varepsilon R)\Big)\chi_{\{\rho-r>0\}} \\ & +\frac{I_{|n|}(\omega_\varepsilon r_<)}{I_{|n|}(\omega_\varepsilon R)}\Big(I_{|n|}(\omega_\varepsilon R)K'_{|n|}(\omega_\varepsilon r_>) - I'_{|n|}(\omega_\varepsilon r_>)K_{|n|}(\omega_\varepsilon R)\Big)\delta(r-\rho)\Bigg\}\cos(n(\theta-\psi))\end{aligned}$$

which, thanks again to the Wronskian relation (2.21), yields,

$$\boxed{\frac{\partial^2 H_\varepsilon^0}{\partial\rho\partial r}(0,\theta;R,\psi) = -\frac{\omega_\varepsilon\,\cos(\psi-\theta)}{2\pi R\, I_1(\omega_\varepsilon R)}.} \tag{2.22}$$

Now, we are ready to compute the mixed derivative for G_ε^0 in (2.9), evaluated at $r=0, \rho=R$. Thanks to the Dirichlet boundary conditions imposed on G_ε in (2.11),

$$-\frac{\partial^2 G_\varepsilon^0}{\partial\rho\partial r}(r=0,\theta;\rho=R,\psi) = \frac{\omega_\varepsilon \exp(-\omega_\varepsilon R\cos(\psi-\mu))}{2\pi R}\left(\frac{\cos(\theta-\mu)}{I_0(\omega_\varepsilon R)} + \frac{\cos(\theta-\psi)}{I_1(\omega_\varepsilon R)}\right),$$

which ends the proof using (2.9). □

Remark 1 (special case of Poisson's potential). *Since $I_1(z)\to z/2$ as $z\to 0$, it comes that the "mixed derivative" evaluated at $r=0,\rho=R$ satisfies,*

$$\frac{\partial^2 H_\varepsilon^0}{\partial\rho\partial r}(0,\theta;R,\psi) = \frac{\omega_\varepsilon\,\cos(\psi-\theta)}{2\pi R\, I_1(\omega_\varepsilon R)} \to \frac{\cos(\psi-\theta)}{\pi R^2} \quad \text{when } \omega_\varepsilon \to 0.$$

This result is coherent with the Poisson kernel, [11]: indeed, if $\mathbf{V}\equiv\vec{0}$ and $\varepsilon=1$,

$$u(r,\theta) = \frac{1}{2\pi}\int_0^{2\pi} h(\psi)\mathbb{P}(r,\theta,R,\psi)\,\mathrm{d}\psi, \quad \mathbb{P} = \frac{R^2-r^2}{R^2-2Rr\cos(\theta-\psi)+r^2}.$$

By computing the corresponding r-derivative, one gets

$$\left.\frac{\partial\mathbb{P}}{\partial r}\right|_{r=0} = \frac{2\cos(\theta-\psi)}{R}, \qquad \frac{\partial u}{\partial r}(r=0,\theta) = \frac{1}{\pi R}\int_0^{2\pi} h(\psi)\cos(\theta-\psi)\,\mathrm{d}\psi, \tag{2.23}$$

which agrees with (2.9) as soon as the limit $\omega_\varepsilon\to 0$ of (2.22) is taken.

Moreover, we can take advantage of the "double-layer potential" value of u in (2.8) at $r=0$. Thanks again to the Dirichlet boundary conditions,

$$\frac{\partial G_\varepsilon^0}{\partial\rho}(0,\theta;R,\psi) = -\frac{\exp(-\omega_\varepsilon\,\cos(\psi-\mu)R)}{2\pi R\, I_0(\omega R)},$$

which yields a formula used in [15, eqn. (3.2)],

$$u(r=0,\theta) = \frac{\varepsilon}{I_0(\omega_\varepsilon R)}\int_0^{2\pi} h(\psi)\exp(-\omega_\varepsilon\,\cos(\psi-\mu)R)\,\frac{\mathrm{d}\psi}{2\pi}. \tag{2.24}$$

Accordingly,

$$\boxed{\frac{\partial u}{\partial r}(0,\theta) = \varepsilon\left(\omega_\varepsilon\cos(\theta-\mu)u(0,\theta) + \frac{\omega_\varepsilon}{I_1(\omega_\varepsilon R)}\int_0^{2\pi} h(\psi)E(\psi)\cos(\theta-\psi)\,\frac{\mathrm{d}\psi}{2\pi}\right),}$$

which splits naturally between a "transport part" and a "diffusive part", as we will see later in details. More precisely, here we define the "transport term" as follows,

$$T^\mu(\theta) = \frac{\omega_\varepsilon\,\cos(\theta-\mu)}{2\pi\, I_0(\omega_\varepsilon R)}\int_0^{2\pi} h(\psi)\exp(-\omega_\varepsilon R\cos(\psi-\mu))\,\mathrm{d}\psi, \tag{2.25}$$

while the "diffusive term" reads,

$$D^\mu(\theta) = \frac{\omega_\varepsilon}{2\pi I_1(\omega_\varepsilon R)}\int_0^{2\pi} h(\psi)\exp(-\omega_\varepsilon R\cos(\psi-\mu))\cos(\theta-\psi)\,\mathrm{d}\psi. \tag{2.26}$$

Numerical fluxes will be retrieved from both (2.25) and (2.26) by approximating $h(\psi)$.

3. Practical derivation of 2D fluxes. Beside the Poisson kernel, recovered for $\varepsilon = 1$, $\mathbf{V} = \vec{0}$, the general behavior of these radial derivatives is now studied;

$$\forall n \in \mathbb{N}, x \in \mathbb{R}, \qquad I_n(x) = \frac{1}{\pi} \int_0^\pi \exp(x \cos\psi) \cos n\psi \, \mathrm{d}\psi. \tag{3.1}$$

This is called the "*integral representation of modified Bessel functions*", [1]. Another integral representation of modified Bessel functions is as follows,

$$\forall n \in \mathbb{N}, x \in \mathbb{R}, \quad I_n(x) = \frac{(x/2)^n}{\sqrt{\pi}\,\Gamma(n+\frac{1}{2})} \int_0^\pi \exp(x\cos\psi) |\sin\psi|^{2n} \, \mathrm{d}\psi. \tag{3.2}$$

This formula is easy for $n = 0, 1$ because $\Gamma(\frac{1}{2}) = \sqrt{\pi}$, $\Gamma(\frac{3}{2}) = \frac{\sqrt{\pi}}{2}$, so that,

$$\forall x \neq 0, \qquad \frac{I_1(x)}{x} = \int_0^\pi \exp(x\cos\psi) |\sin\psi|^2 \, \frac{\mathrm{d}\psi}{\pi}.$$

3.1. Trigonometric polynomial approximation of $h(\psi)$. Denote $x_i = i\Delta x, y_j = j\Delta x$, for $i, j \in \mathbb{Z}^2$: at any time-step $t^n = n\Delta t$, we only have a set of discrete values at hand; in particular, instead of knowing the boundary data on each circle C, we are just aware of 4 discrete points, so we must deduce boundary data $h(\psi)$ from a "trigonometric polynomial interpolation" of discrete ones $u^n_{i,j} \simeq u(t^n, x_i, y_j)$ available on the uniform Cartesian grid. Accordingly, the most natural manner of deducing a trigonometric polynomial out of 4 values $u^n_{i,j}, u^n_{i-1,j}, u^n_{i-1,j-1}, u^n_{i,j-1}$,

$$h_4(\psi) = \mathbf{a}_0 + \mathbf{a}_1 \cos\psi + \mathbf{b}_1 \sin\psi + \mathbf{a}_2 \cos 2\psi + b_2 \sin 2\psi, \quad \psi \in (0, 2\pi), \tag{3.3}$$

so that

$$h_4(0) = u^n_{i,j},\ h_4(\frac{\pi}{2}) = u^n_{i-1,j},\ h_4(\pi) = u^n_{i-1,j-1},\ h_4(\frac{3\pi}{2}) = u^n_{i,j-1}.$$

Fourier coefficients follow from inverting the linear system,

$$\begin{aligned}
\mathbf{a}_0 &= \frac{1}{4}(u^n_{i,j} + u^n_{i-1,j} + u^n_{i-1,j-1} + u^n_{i,j-1}),\\
\mathbf{a}_1 &= \frac{1}{2}(u^n_{i,j} - u^n_{i-1,j-1}), \qquad \mathbf{b}_1 = \frac{1}{2}(u^n_{i-1,j} - u^n_{i,j-1}),\\
\mathbf{a}_2 &= \frac{1}{4}(u^n_{i,j} + u^n_{i-1,j-1}) - \frac{1}{4}(u^n_{i-1,j} + u^n_{i,j-1}).
\end{aligned} \tag{3.4}$$

For a disk of radius $R = \frac{\Delta x}{\sqrt{2}}$, numerical fluxes are given by (2.23),

$$\frac{\partial u}{\partial r}(r = 0, \theta = 0) = \frac{\sqrt{2}}{\pi\Delta x} \int_0^{2\pi} h_4(\psi) \cos\psi \, \mathrm{d}\psi.$$

The reason why we compute the radial derivative in the direction $\theta = 0$ is because we fixed the origin of the angles $\psi = 0$ in x_i, y_j and the Laplacian is invariant by rotation. Otherwise, there would be a shift of $\frac{\pi}{4}$ everywhere. By orthogonality, only $\mathbf{a}_1$ contributes to the overall flux value at the center of the disk:

$$\frac{\partial u}{\partial r}(r = 0, \theta = 0) = \frac{\mathbf{a}_1}{\pi R} \int_0^{2\pi} \cos^2\psi \, \mathrm{d}\psi = \frac{\mathbf{a}_1}{\pi R} \left[\frac{\psi}{2} + \frac{\sin\psi\cos\psi}{2} \right]_0^{2\pi}.$$

In order to get the final expression of the time-marching scheme,

$$\begin{aligned}\frac{u_{i,j}^{n+1}-u_{i,j}^{n}}{\Delta t} =&\frac{1}{2R}\left[\left(\frac{\mathbf{a}_1}{R}\right)_{i+\frac12,j+\frac12}-\left(\frac{\mathbf{a}_1}{R}\right)_{i-\frac12,j-\frac12}+\left(\frac{\mathbf{b}_1}{R}\right)_{i-\frac12,j+\frac12}-\left(\frac{\mathbf{b}_1}{R}\right)_{i+\frac12,j-\frac12}\right]\\ =&\frac{1}{4R^2}\left(-4u_{i,j}^n+u_{i-1,j-1}^n+u_{i+1,j+1}^n+u_{i-1,j+1}^n+u_{i+1,j-1}^n\right),\end{aligned}$$

and the resulting "diagonal nodal scheme" is both monotone (under standard parabolic CFL restriction) and consistent (because $4R^2 = 2\Delta x^2$).

3.2. Transport and diffusion terms in the radial derivative. Given an angle $\mu \in (-\pi, \pi)$ as in (2.12), we can write a 4-points approximation T_4^μ of T^μ by inserting (3.3) into (2.25) and computing exactly the resulting integral thanks to (3.1). Yet, by expanding the trigonometric terms, using the orthogonality of the Fourier basis and the properties of the Bessel functions, one finds:

LEMMA 3.1.

$$T_4^\mu(\theta)=\omega_\varepsilon\cos(\theta-\mu)\left(\boldsymbol{a}_0-\left(\boldsymbol{a}_1\cos\mu+\boldsymbol{b}_1\sin\mu\right)\frac{I_1(\omega_\varepsilon R)}{I_0(\omega_\varepsilon R)}+\boldsymbol{a}_2\cos 2\mu\frac{I_2(\omega_\varepsilon R)}{I_0(\omega_\varepsilon R)}\right) \tag{3.5}$$

Proof. Assume first that boundary data is a simpler trigonometric polynomial,

$$\forall\psi\in(0,2\pi),\qquad h_3(\psi)=\mathbf{a}_0+\mathbf{a}_1\cos\psi+\mathbf{b}_1\sin\psi,$$

then, given an angle $\mu \in (0, 2\pi)$, and denoting

$$\begin{aligned}T_3^\mu(\theta)&=\frac{\omega_\varepsilon\ \cos(\theta-\mu)}{2\pi\, I_0(\omega_\varepsilon R)}\int_0^{2\pi}h_3(\psi)\exp(-\omega_\varepsilon R\cos(\psi-\mu))\,\mathrm{d}\psi\\ &=\frac{\omega_\varepsilon\ \cos(\theta-\mu)}{2\pi\, I_0(\omega_\varepsilon R)}\int_0^{2\pi}h_3(\psi+\mu)\exp(-\omega_\varepsilon R\cos\psi)\,\mathrm{d}\psi\\ &=\frac{\omega_\varepsilon\ \cos(\theta-\mu)}{2\pi\, I_0(\omega_\varepsilon R)}\int_0^{2\pi}\big(\mathbf{a}_0+\mathbf{a}_1\cos(\psi+\mu)+\mathbf{b}_1\sin(\psi+\mu)\big)\exp(-\omega_\varepsilon R\cos\psi)\,\mathrm{d}\psi.\end{aligned}$$

Yet, by expanding the trigonometric terms,

$$\cos(\psi+\mu)=\cos\psi\cos\mu-\sin\psi\sin\mu,\quad \sin(\psi+\mu)=\sin\psi\cos\mu+\cos\psi\sin\mu,$$

one gets cancellations because, by periodicity,

$$\int_0^{2\pi}\exp(-\omega_\varepsilon R\cos\psi)\sin\psi\,\mathrm{d}\psi=\left[-\frac{\exp(-\omega_\varepsilon R\cos\psi)}{\omega_\varepsilon R}\right]_0^{2\pi}=0.$$

Accordingly, remaining terms read:

$$\mathbf{a}_0\int_0^{2\pi}\exp(-\omega_\varepsilon R\cos\psi)\,\frac{\mathrm{d}\psi}{2\pi}=\mathbf{a}_0\, I_0(\omega_\varepsilon R),$$

and since $I_1(-x) = -I_1(x)$, (because for any $n \in \mathbb{N}$, $I_n(-x) = (-1)^n\, I_n(x)$)

$$\mathbf{a}_1\int_0^{2\pi}\cos(\psi+\mu)\exp(-\omega_\varepsilon R\cos\psi)\,\frac{\mathrm{d}\psi}{2\pi}=-\mathbf{a}_1\, I_1(\omega_\varepsilon R)\,\cos\mu.$$

by (3.1),

$$T_3^\mu(\theta) = \omega_\varepsilon\ \cos(\theta-\mu)\left(\mathbf{a}_0 - (\mathbf{a}_1\cos\mu + \mathbf{b}_1\sin\mu)\frac{I_1(\omega_\varepsilon R)}{I_0(\omega_\varepsilon R)}\right).$$

Then, with the "4-points trigonometric polynomial" (3.3), a new term will appear,

$$\cos(2(\psi+\mu)) = \cos 2\psi\cos 2\mu - 2\sin\psi\cos\psi\sin 2\mu, \tag{3.6}$$

where

$$\forall a\in\mathbb{R}, \qquad \int_0^{2\pi}\exp(a\cos\psi)\sin\psi\cos\psi\,\mathrm{d}\psi = 0.$$

Using (3.6) along with the relation, $\cos(2\psi) = \cos^2\psi - \sin^2\psi = 1 - 2\sin^2\psi$,

$$\begin{aligned}
&\frac{\omega_\varepsilon\cos(\theta-\mu)\cos(2\mu)\mathbf{a}_2}{I_0(\omega_\varepsilon R)}\int_0^{2\pi}\cos(2\psi)\exp(-\omega_\varepsilon R\cos\psi)\,\frac{\mathrm{d}\psi}{2\pi}\\
&\quad= \frac{\omega_\varepsilon\cos(\theta-\mu)\cos(2\mu)\mathbf{a}_2}{I_0(\omega_\varepsilon R)}\left[I_0(\omega_\varepsilon R) - \frac{2I_1(\omega_\varepsilon R)}{\omega_\varepsilon R}\right]\\
&\quad= \omega_\varepsilon\cos(\mu-\theta)\cos(2\mu)\mathbf{a}_2\left[1 - \frac{2I_1(\omega_e R)}{\omega_\varepsilon R I_0(\omega_\varepsilon R)}\right].
\end{aligned}$$

The integral equality (3.1) gives

$$\begin{aligned}
&\frac{\omega_\varepsilon\cos(\theta-\mu)\cos(2\mu)\mathbf{a}_2}{I_0(\omega_\varepsilon R)}\int_0^{2\pi}\cos(2\psi)\exp(-\omega_\varepsilon R\cos\psi)\,\frac{\mathrm{d}\psi}{2\pi}\\
&\qquad\qquad= \frac{\omega_\varepsilon\cos(\theta-\mu)\cos(2\mu)I_2(\omega_\varepsilon R)\mathbf{a}_2}{I_0(\omega_\varepsilon R)}.
\end{aligned}$$

Former calculations yield, in a very similar manner, the expression (3.5). ◻ Analogously, the following lemma holds.

LEMMA 3.2. *The 4-points approximation D_4^μ of D^μ in (2.26) is given by:*

$$\begin{aligned}
D_4^\mu(\theta) =\omega_\varepsilon\Bigg(&\cos(\theta-\mu)\left\{-\boldsymbol{a}_0 + (\boldsymbol{a}_1\cos\mu + \boldsymbol{b}_1\sin\mu)\frac{I_0(\omega_\varepsilon R)}{I_1(\omega_\varepsilon R)} - \boldsymbol{a}_2\cos 2\mu\right\}\\
&+\frac{-\boldsymbol{a}_1\cos(\theta-2\mu) + \boldsymbol{b}_1\sin(\theta-2\mu)}{\omega_\varepsilon R}\Bigg).
\end{aligned}\tag{3.7}$$

Proof. Again, consider first the simpler case where $h(\psi) = h_3(\psi)$,

$$\begin{aligned}
D_3^\mu(\theta) &= \frac{\omega_\varepsilon}{I_1(\omega_\varepsilon R)}\int_0^{2\pi} h_3(\psi+\mu)\exp(-\omega_\varepsilon R\cos\psi)\cos(\psi+(\mu-\theta))\,\frac{\mathrm{d}\psi}{2\pi}\\
&= \frac{\omega_\varepsilon}{I_1(\omega_\varepsilon R)}\int_0^{2\pi}\big(\mathbf{a}_0 + \mathbf{a}_1\cos(\psi+\mu) + \mathbf{b}_1\sin(\psi+\mu)\big)\\
&\qquad\qquad\times\exp(-\omega_\varepsilon R\cos\psi)\cos\big(\psi+(\mu-\theta)\big)\,\frac{\mathrm{d}\psi}{2\pi}.
\end{aligned}$$

The integral associated to the constant term $\mathbf{a}_0$ is easy:

$$\frac{\mathbf{a}_0\,\omega_\varepsilon}{I_1(\omega_\varepsilon R)}\int_0^{2\pi}\exp(-\omega_\varepsilon R\cos\psi)\cos\big(\psi+(\mu-\theta)\big)\,\frac{\mathrm{d}\psi}{2\pi}=-\mathbf{a}_0\cos(\mu-\theta)\omega_\varepsilon.$$

Yet, both terms multiplied by $\mathbf{a}_1$ and $\mathbf{b}_1$ can be handled the same way:

- the product $\cos(\psi+\mu)\cos(\psi+\mu-\theta)$ yields,

  $$\cos^2\psi\cos\mu\cos(\mu-\theta)+\sin^2\psi\sin\mu\sin(\mu-\theta)-\sin\psi\cos(\psi)(...),$$

  where the "mixed" terms $\sin\psi\cos\psi(...)=\sin 2\psi(...)$ vanish, since they are orthogonal in the scalar product induced by $\exp(-\omega_\varepsilon R\cos\psi)$ in $L^2([0,2\pi])$. It is interesting to rewrite the first product as,

  $$\cos\mu\cos(\mu-\theta)-\big(\cos\mu\cos(\mu-\theta)-\sin\mu\sin(\mu-\theta)\big)\sin^2\psi,$$

  so that, using (3.2), the integral becomes:

  $$\begin{aligned}&\frac{\mathbf{a}_1\,\omega_\varepsilon}{I_1(\omega_\varepsilon R)}\int_0^{2\pi}\cos(\psi+\mu)\exp(-\omega_\varepsilon R\cos\psi)\cos\big(\psi+(\mu-\theta)\big)\,\frac{\mathrm{d}\psi}{2\pi}\\ =&\frac{\mathbf{a}_1\,\omega_\varepsilon}{I_1(\omega_\varepsilon R)}\Bigg(\cos\mu\cos(\mu-\theta)\int_0^{2\pi}\exp(-\omega_\varepsilon R\cos\psi)\,\frac{\mathrm{d}\psi}{2\pi}\\ &\qquad-\cos(2\mu-\theta)\int_0^{2\pi}\exp(-\omega_\varepsilon R\cos\psi)\sin^2\psi\,\frac{\mathrm{d}\psi}{2\pi}\Bigg)\\ =&\frac{\mathbf{a}_1\,\omega_\varepsilon}{I_1(\omega_\varepsilon R)}\Bigg(\cos\mu\cos(\mu-\theta)I_0(\omega_\varepsilon R)-\cos(2\mu-\theta)\frac{I_1(-\omega_\varepsilon R)}{-\omega_\varepsilon R}\Bigg);\end{aligned}$$

- similarly, explicitly solving the product $\sin(\psi+\mu)\cos(\psi+\mu-\theta)$ and, using (3.2), the integral reads,

  $$\begin{aligned}&\frac{\mathbf{b}_1\,\omega_\varepsilon}{I_1(\omega_\varepsilon R)}\int_0^{2\pi}\sin(\psi+\mu)\exp(-\omega_\varepsilon R\cos\psi)\cos\big(\psi+(\mu-\theta)\big)\,\frac{\mathrm{d}\psi}{2\pi}\\ =&\frac{\mathbf{b}_1\,\omega_\varepsilon}{I_1(\omega_\varepsilon R)}\Bigg(\sin\mu\cos(\mu-\theta)\int_0^{2\pi}\exp(-\omega_\varepsilon R\cos\psi)\,\frac{\mathrm{d}\psi}{2\pi}\\ &\qquad-\sin(2\mu-\theta)\int_0^{2\pi}\exp(-\omega_\varepsilon R\cos\psi)\sin^2\psi\,\frac{\mathrm{d}\psi}{2\pi}\Bigg)\\ =&\frac{\mathbf{b}_1\,\omega_\varepsilon}{I_1(\omega_\varepsilon R)}\Bigg(\sin\mu\cos(\mu-\theta)I_0(\omega_\varepsilon R)-\sin(2\mu-\theta)\frac{I_1(-\omega_\varepsilon R)}{-\omega_\varepsilon R}\Bigg).\end{aligned}$$

Accordingly, using $I_1(-x)=-I_1(x)$, diffusive 3-points fluxes read:

$$\begin{aligned}D_3^\mu(\theta)=\omega_\varepsilon\Bigg(&\cos(\theta-\mu)\left\{-\mathbf{a}_0+(\mathbf{a}_1\cos\mu+\mathbf{b}_1\sin\mu)\frac{I_0(\omega_\varepsilon R)}{I_1(\omega_\varepsilon R)}\right\}\\ &-\frac{\mathbf{a}_1\cos(\theta-2\mu)+\mathbf{b}_1\sin(\theta-2\mu)}{\omega_\varepsilon R}\Bigg).\end{aligned}$$

To treat the "4-points trigonometric polynomial" $h_4(\psi)$, it remains to consider

$$\begin{aligned}\cos(2\psi+2\mu)\cos(\psi+\mu-\theta)&=\cos 2\psi\cos\psi\cos 2\mu\cos(\mu-\theta)\\ +\sin 2\psi\sin\psi\sin 2\mu\sin(\mu-\theta)&-\cos 2\psi\sin\psi\cos 2\mu\sin(\mu-\theta)\\ &-\sin 2\psi\cos\psi\sin 2\mu\cos(\mu-\theta).\end{aligned}$$

As before, in the integrals corresponding to mixed terms, *e.g.*, $\cos 2\psi \sin\psi$,

$$D_4^\mu(\theta) = \frac{\omega_\varepsilon}{I_1(\omega_\varepsilon R)} \int_0^{2\pi} \big(\mathbf{a}_0 + \mathbf{a}_1 \cos(\psi+\mu) + \mathbf{b}_1 \sin(\psi+\mu) \\ + \mathbf{a}_2 \cos(2\psi + 2\mu)\big) \exp(-\omega_\varepsilon R \cos\psi) \cos\big(\psi + (\mu-\theta)\big) \frac{\mathrm{d}\psi}{2\pi},$$

it suffices to deal only with supplementary non-zero coefficients related to $\mathbf{a}_2$,

$$\begin{aligned} &\frac{\omega_\varepsilon\, \mathbf{a}_2\, \cos 2\mu \cos(\mu-\theta)}{I_1(\omega_\varepsilon\, R)} \Bigg[\int_0^{2\pi} \cos 2\psi \cos\psi \exp(-\omega_\varepsilon R\cos\psi)\, \frac{\mathrm{d}\psi}{2\pi} \\ &\qquad + \int_0^{2\pi} \sin 2\psi \sin\psi \exp(-\omega_\varepsilon R \cos\psi)\, \frac{\mathrm{d}\psi}{2\pi} \Bigg] \\ &= \frac{\omega_\varepsilon\, \mathbf{a}_2\, \cos 2\mu \cos(\mu-\theta)}{I_1(\omega_\varepsilon\, R)} \int_0^{2\pi} \cos\psi \exp(-\omega_\varepsilon R\cos\psi)\, \frac{\mathrm{d}\psi}{2\pi} \\ &= -\omega_\varepsilon \cos(\mu-\theta)\, \mathbf{a}_2 \cos 2\mu. \end{aligned}$$

□

4. Some properties of the resulting "fully 2D" scheme.

4.1. Incremental (Harten) coefficients. From (3.4) and Lemmas 3.1 & 3.2, the resulting 2D fluxes read: for any $\theta = k\pi/2$, with $k \in \mathbb{N}$,

$$T_4^\mu(\theta) - D_4^\mu(\theta) = \Bigg\{ 2\mathbf{a}_0 - (\mathbf{a}_1 \cos\mu + \mathbf{b}_1 \sin\mu) \left(\frac{I_1}{I_0}(\omega_\varepsilon R) + \frac{I_0}{I_1}(\omega_\varepsilon R) - \frac{1}{\omega_\varepsilon R} \right) \\ + \mathbf{a}_2 \cos(2\mu) \left(1 + \frac{I_2}{I_0}(\omega_\varepsilon R) \right) \Bigg\} \omega_\varepsilon \cos(\theta-\mu) + \frac{(\mathbf{a}_1 \sin\mu - \mathbf{b}_1 \cos\mu)\sin(\theta-\mu)}{R},$$

where $\omega_\varepsilon := |\mathbf{V}|/2\varepsilon$, see (2.12). Yet. inserting generic Fourier coefficients,

$$\mathbf{a}_0 = \frac{a+b+c+d}{4}, \quad \mathbf{a}_1 = \frac{c-d}{2}, \quad \mathbf{b}_1 = \frac{a-b}{2}, \quad \mathbf{a}_2 = \frac{c+d}{4} - \frac{a+b}{4},$$

yields the following expression:

$$\begin{aligned} T_4^\mu(\theta) - D_4^\mu(\theta) = &\left(\frac{(c-d)\sin\mu}{2} - \frac{(a-b)\cos\mu}{2} \right) \frac{\sin(\theta-\mu)}{R} + \Bigg\{ \frac{a+b+c+d}{2} \\ &- \left(\frac{(c-d)\cos\mu}{2} + \frac{(a-b)\sin\mu}{2} \right) \left(\frac{I_1}{I_0}(\omega_\varepsilon R) + \frac{I_0}{I_1}(\omega_\varepsilon R) - \frac{1}{\omega_\varepsilon R} \right) \\ &+ \left(\frac{c+d}{4} - \frac{a+b}{4} \right) \cos(2\mu) \left(1 + \frac{I_2}{I_0}(\omega_\varepsilon R) \right) \Bigg\} \omega_\varepsilon \cos(\theta-\mu). \end{aligned}$$

We now intend to make incremental (Harten) coefficients explicit:

$$
\begin{aligned}
T_4^\mu(\theta) - D_4^\mu(\theta) =& a\,\mathcal{C}_a^\mu(\theta) + b\,\mathcal{C}_b^\mu(\theta) + c\,\mathcal{C}_c^\mu(\theta) + d\,\mathcal{C}_d^\mu(\theta) := \frac{\omega_\varepsilon \cos(\theta-\mu)}{2} \times \\
&\left[a\left\{1 - \sin\mu\,\mathcal{B}_1(\omega_\varepsilon R) - \frac{\cos(2\mu)}{2}\,\mathcal{B}_2(\omega_\varepsilon R) - \frac{\cos\mu\tan(\theta-\mu)}{\omega_\varepsilon\,R}\right\} + \right.\\
&b\left\{1 + \sin\mu\,\mathcal{B}_1(\omega_\varepsilon R) - \frac{\cos(2\mu)}{2}\,\mathcal{B}_2(\omega_\varepsilon R) + \frac{\cos\mu\tan(\theta-\mu)}{\omega_\varepsilon\,R}\right\} + \\
&c\left\{1 - \cos\mu\,\mathcal{B}_1(\omega_\varepsilon R) + \frac{\cos(2\mu)}{2}\,\mathcal{B}_2(\omega_\varepsilon R) + \frac{\sin\mu\tan(\theta-\mu)}{\omega_\varepsilon\,R}\right\} + \\
&\left.d\left\{1 + \cos\mu\,\mathcal{B}_1(\omega_\varepsilon R) + \frac{\cos(2\mu)}{2}\,\mathcal{B}_2(\omega_\varepsilon R) - \frac{\sin\mu\tan(\theta-\mu)}{\omega_\varepsilon\,R}\right\}\right],
\end{aligned}
$$

where

$$
\mathcal{B}_1(\omega_\varepsilon R) = \left(\frac{I_1}{I_0} + \frac{I_0}{I_1}\right)(\omega_\varepsilon R) - \frac{1}{\omega_\varepsilon R} \in (1.6, +\infty), \qquad \mathcal{B}_2(\omega_\varepsilon R) = 1 + \frac{I_2}{I_0}(\omega_\varepsilon R) \geq 1.
$$

A few (obvious) observations are:

- let $a = b = c = d$, so that incremental coefficients add each other, it comes
$$
\forall\theta,\mu, \qquad T_4^\mu(\theta) - D_4^\mu(\theta) = 2\omega_\varepsilon\, a\cos(\theta-\mu) = a\,\frac{|\mathbf{V}|}{\varepsilon}\cos(\theta-\mu).
$$
- let $\varepsilon = 1$ and $(\omega R, \mu) \to 0$ (purely diffusive limit): when $0 \leq x \ll 1$,
$$
\forall n \in \mathbb{N}, \qquad I_n(x) = \frac{1}{n!}\left(\frac{x}{2}\right)^n + O(x^2), \qquad \text{so} \qquad \frac{I_1}{I_0} + \frac{I_0}{I_1}(\omega R) - \frac{1}{\omega R} \simeq \frac{1}{\omega R}.
$$
  Numerical fluxes reduce to,
$$
T_4^0(\theta) - D_4^0(\theta) \simeq -\frac{(a-b)\sin\theta + (c-d)\cos\theta}{2R},
$$
  so that a diagonal, centered (2nd order), 5-points scheme is recovered.
- more generally, let $\mu = 0, \varepsilon = 1$ and the (fine-grid) regime be $0 \leq \omega R \ll 1$:
$$
\begin{aligned}
T_4^0(\theta) - D_4^0(\theta) \simeq &\left[a\left(\frac{\omega\cos\theta}{4} - \frac{\sin\theta}{2R}\right) + b\left(\frac{\omega\cos\theta}{4} + \frac{\sin\theta}{2R}\right)\right. \qquad (4.1)\\
&\left. + c\left(\frac{3\omega\cos\theta}{4} - \frac{\cos\theta}{2R}\right) + d\left(\frac{3\omega\cos\theta}{4} + \frac{\cos\theta}{2R}\right)\right].
\end{aligned}
$$
  The (centered) average is biased along the flow's direction.

4.2. Asymptotic properties and directional monotony as $\varepsilon \to 0$. On the contrary, one may consider "transport-dominant" (or "vanishing viscosity") asymptotic regimes for which $\omega_\varepsilon R \gg 1$, and study the behavior of rescaled 2D fluxes:

$$
\forall\theta,\mu, \qquad F^\mu(\theta) := \varepsilon\big(T_4^\mu(\theta) - D_4^\mu(\theta)\big).
$$

A crucial property of modified Bessel functions $I_n(x)$ is,

$$
\forall(n,m) \in \mathbb{N}^2, \qquad \lim_{x\to+\infty} \frac{I_n(x)}{I_m(x)} = 1,
$$

so that, asymptotically as $\varepsilon \to 0$, our rescaled 2D fluxes boil down to:

$$\begin{aligned} F^\mu(\theta) :=& \varepsilon\big(T_4^\mu(\theta) - D_4^\mu(\theta)\big) \\ =& \frac{\omega\cos(\theta-\mu)}{2}\Big[a\Big\{1 - 2\sin\mu - \cos(2\mu) - O(\varepsilon)\Big\} \\ &\qquad + b\Big\{1 + 2\sin\mu - \cos(2\mu) + O(\varepsilon)\Big\} \\ &\qquad\quad + c\Big\{1 - 2\cos\mu + \cos(2\mu) + O(\varepsilon)\Big\} \\ &\qquad\qquad + d\Big\{1 + 2\cos\mu + \cos(2\mu) - O(\varepsilon)\Big\}\Big]. \end{aligned}$$

At this point, it is convenient to state:

Definition 1. *Given a grid parameter $\Delta x > 0$, a numerical scheme is called "asymptotically monotone" (under a certain CFL restriction) as $\varepsilon \to 0$ when the limiting values of all its incremental coefficients are nonnegative.*

Assume $0 < \omega, \mu$ are constants given in the whole computational domain, so that the drift-diffusion equation becomes an advection-diffusion one (like in [15, 19, 24]). The most direct way to discretize the resulting problem is, in standard notation,

$$u_{i,j}^{n+1} = u_{i,j}^n + \frac{\Delta t}{2R}\left(F^\mu_{i-\frac12,j-\frac12}(0) + F^\mu_{i+\frac12,j+\frac12}(\pi) + F^\mu_{i+\frac12,j-\frac12}(\frac{\pi}{2}) + F^\mu_{i-\frac12,j+\frac12}(-\frac{\pi}{2})\right). \tag{4.2}$$

A basic result is:

Lemma 1. *Let $\mu = k\frac{\pi}{2}$, $k \in \mathbb{N}$, so that the flow is diagonal, then (4.2) preserves the total mass and is asymptotically monotone as $\varepsilon \to 0$ under the CFL restriction,*

$$\left[\frac{\varepsilon}{R} + \omega\mathcal{B}_1(\omega_\varepsilon R)\right]\Delta t = \left[\frac{\varepsilon}{R} + \omega\left(\frac{I_1}{I_0} + \frac{I_0}{I_1}(\omega_\varepsilon R) - \frac{\varepsilon}{\omega R}\right)\right]\Delta t \le 2R. \tag{4.3}$$

Proof. Only the case $\mu = 0$ is studied as the other ones are similar. Total mass preservation is ensured by the incremental coefficients adding to unity, which is clear from the definition of each $F^\mu(\theta)$. Beside, the restriction (4.3) is obtained by ensuring positivity of the coefficient acting on $u^n_{i,j}$. Finally, consider the limit $\varepsilon \to 0, \mu = 0$ in

$$F^0(\theta) = \frac{\omega}{2}\cos\theta\,\big(O(\varepsilon)(a+b+c+d) + 4d\big) = 2\omega\cos\theta\, d,$$

which is the expression of a (diagonal) upwind scheme, obviously monotone. □

We aim at getting asymptotic monotony for both horizontal and vertical flows, too, but it is quite easy to see that it doesn't hold unless a viscous correction is added. Accordingly, define

$$\begin{aligned} u_{i,j}^{n+1} = u_{i,j}^n &+ \frac{\Delta t}{2R}\left(F^\mu_{i-\frac12,j-\frac12}(0) + F^\mu_{i+\frac12,j+\frac12}(\pi) + F^\mu_{i+\frac12,j-\frac12}(\frac{\pi}{2}) + F^\mu_{i-\frac12,j+\frac12}(-\frac{\pi}{2})\right) \\ &+ \frac{\omega\Delta t}{4R}\max\left(0, \frac{I_1}{I_0}(\omega_\varepsilon R)\sin 2\mu\right)\Big((u^n_{i+1,j} - u^n_{i,j}) - (u^n_{i,j} - u^n_{i-1,j})\Big) \\ &+ \frac{\omega\Delta t}{4R}\max\left(0, -\frac{I_1}{I_0}(\omega_\varepsilon R)\sin 2\mu\right)\Big((u^n_{i,j+1} - u^n_{i,j}) - (u^n_{i,j} - u^n_{i,j-1})\Big). \end{aligned} \tag{4.4}$$

Lemma 2. *Let $\mu = k\frac{\pi}{4}$, $k \in \mathbb{N}$, then (4.4) preserves the total mass and is asymptotically monotone as $\varepsilon \to 0$ under the CFL restriction,*

$$\left[\frac{\varepsilon}{R\sqrt{2}} + \omega\left(\mathcal{B}_1(\omega_\varepsilon R) + \frac{|\sin 2\mu|}{2}\frac{I_1}{I_0}(\omega_\varepsilon R)\right)\right]\Delta t \le 2R. \tag{4.5}$$

Proof. Since $\sin 2\mu = 0$ for $\mu = k\pi/2$, Lemma 1 still holds because the viscous correction in (4.4) vanishes. Again, we shall check the claims for $\mu = \frac{\pi}{4}$ only as other cases are similar. Now, consider that, for $\mu = \frac{\pi}{4}$, $\sin\mu = \cos\mu = \frac{1}{\sqrt{2}}$ thus,

$$\begin{aligned} F^{\frac{\pi}{4}}(\theta) = &\frac{\varepsilon(\cos\theta - \sin\theta)}{4\,R}\big[(a-b)-(c-d)\big] \\ &+ \frac{\omega}{2\sqrt{2}}(\cos\theta + \sin\theta)\Big[\,(a+c)\Big\{1 - \frac{\mathcal{B}_1(\omega_\varepsilon R)}{\sqrt{2}}\Big\} + (b+d)\Big\{1 + \frac{\mathcal{B}_1(\omega_\varepsilon R)}{\sqrt{2}}\Big\}\Big], \end{aligned} \tag{4.6}$$

so that, as $\varepsilon \to 0$, one gets

$$F^{\frac{\pi}{4}}(\theta) \to \frac{\omega}{2}(\cos\theta + \sin\theta)\cos\mu\left[(a+c)(1-2\sin\mu) + (b+d)(1+2\sin\mu)\right],$$

which yields the sum of resulting fluxes,

$$\begin{aligned} &F^{\mu}_{i-\frac12,j-\frac12}(0) + F^{\mu}_{i+\frac12,j+\frac12}(\pi) + F^{\mu}_{i+\frac12,j-\frac12}(\frac{\pi}{2}) + F^{\mu}_{i-\frac12,j+\frac12}(-\frac{\pi}{2}) \simeq \\ &\quad \frac{\omega}{2}\cos\mu\Big[(u^n_{i,j} + u^n_{i-1,j})(1-2\sin\mu) + (u^n_{i,j-1} + u^n_{i-1,j-1})(1+2\sin\mu) \\ &\qquad - (u^n_{i,j+1} + u^n_{i-1,j+1})(1-2\sin\mu) - (u^n_{i,j} + u^n_{i-1,j})(1+2\sin\mu) \\ &\qquad + (u^n_{i+1,j} + u^n_{i,j})(1-2\sin\mu) + (u^n_{i+1,j-1} + u^n_{i,j-1})(1+2\sin\mu) \\ &\qquad - (u^n_{i+1,j+1} + u^n_{i,j+1})(1-2\sin\mu) - (u^n_{i+1,j} + u^n_{i,j})(1+2\sin\mu)\Big] \\ &\quad \simeq \frac{\omega}{2}\cos\mu\Big[-4u^n_{i,j}\sin\mu - 2(u^n_{i-1,j} + u^n_{i+1,j})\sin\mu \\ &\qquad + (u^n_{i,j-1} + u^n_{i-1,j-1})(1+2\sin\mu) - (u^n_{i,j+1} + u^n_{i-1,j+1})(1-2\sin\mu) \\ &\qquad + (u^n_{i+1,j-1} + u^n_{i,j-1})(1+2\sin\mu) - (u^n_{i+1,j+1} + u^n_{i,j+1})(1-2\sin\mu)\Big]. \end{aligned}$$

In this last expression, only the incremental coefficients acting on $u^n_{i,j}$ and $u^n_{i\pm1,j}$ are negative: in particular the last two ones are

$$-2\cos\mu\sin\mu = -\sin 2\mu,$$

which can be compensated by adding an amount of artificial viscosity like in (4.4). The CFL restriction (4.5) is checked by imposing positivity of the quantity,

$$-\varepsilon\,\Delta t\left[\mathcal{C}^{\mu}_{c}(0) + \mathcal{C}^{\mu}_{d}(\pi) + \mathcal{C}^{\mu}_{a}(\frac{\pi}{2}) + \mathcal{C}^{\mu}_{b}(-\frac{\pi}{2})\right] \leq 2R.$$

Since $\mu = \frac{\pi}{4}$, the sum of the coefficients $\mathcal{C}^{\mu}$'s is $\omega_\varepsilon\mathcal{B}_1(\omega_\varepsilon R) + \frac{1}{R\sqrt{2}}$, to which one must add the viscosity contribution, $\frac{I_1}{I_0}(\omega_\varepsilon R)\frac{|\sin 2\mu|}{2}$: this yields (4.5). □

4.3. Formal second-order accuracy as $\omega R \to 0$. As schemes (4.2) and (4.4) are well-suited for stiff (vanishing viscosity) regimes, we now intend to examine their truncation error in the opposite, fine-grid (diffusion-dominant, or laminar), regime.

THEOREM 1. *Let $\mathbf{V} \in \mathbb{R}^2$ be constant, and $\mu = k\frac{\pi}{4}, k \in \mathbb{N}$: the scheme (4.4) is*

- *second-order in space when $\omega_\varepsilon R \to 0$ and $u(t,\cdot,\cdot) \in C^2$,*
- *asymptotically monotone as $\omega_\varepsilon R \to +\infty$ under (4.5).*

Proof. The second property is a direct consequence of Lemma 2. The first one comes from a study of the scheme's local truncation error; however, for $\mu = k\frac{\pi}{2}, k \in \mathbb{N}$, this is obvious because, according to (4.1), the scheme reduces to a 1D centered discretization along one of the diagonals and the artificial viscosity vanishes:

$$F^0(0) = \frac{\omega_\varepsilon}{4}(a+b) + \frac{3\omega_\varepsilon}{4}(c+d) - \frac{1}{2R}(c-d) = -F^0(\pi),$$
$$F^0(\frac{\pi}{2}) = -\frac{1}{2R}(a-b) = -F^0(-\frac{\pi}{2}),$$

which brings the (diagonally biased) centered scheme,

$$u_{i,j}^{n+1} = u_{i,j}^n + \frac{\varepsilon \Delta t}{2R}\left\{\frac{u_{i+1,j+1}^n + u_{i-1,j-1}^n + u_{i-1,j+1}^n + u_{i+1,j-1}^n - 4u_{i,j}^n}{2R}\right.$$
$$\left. - \frac{\omega_\varepsilon}{4}\Big((u_{i,j+1}^n + u_{i+1,j}^n) - (u_{i-1,j}^n + u_{i,j-1}^n)\Big) - \frac{3\omega_\varepsilon}{4}\big(u_{i+1,j+1}^n - u_{i-1,j-1}^n\big)\right\}.$$

Yet, for $\mu = \frac{\pi}{4}, k \in \mathbb{N}$, the artificial viscosity term is $O(R^2)$ because $\frac{I_1}{I_0}(x) = O(x)$ and Δu is bounded. By computing Taylor expansions in (4.6) for $\omega R \to 0$,

$$F^{\frac{\pi}{4}}(\theta) \simeq \frac{\omega}{4}(a+b+c+d)\sqrt{2} + \frac{(d-c)\cos\theta + (b-a)\sin\theta}{2R}.$$

We recognize the centered flux on the transport term, along with another (diagonal) one on the diffusion. Asymptotic monotony is ensured by the viscous term in (4.4). □

5. Numerical results on 2D Navier-Stokes equations. Most of our practical benchmarks concern the 2D incompressible Navier-Stokes equations (1.3) in vorticity/stream formulation; in particular, boundary conditions are implemented following the classical Thom's formulas (see e.g. [20]). Usually, 2D "uniformly accurate" methods are tested on simpler problems, like advection-diffusion, [24, 29].

5.1. A preliminary drift-diffusion test. Let $V(x,y) \in C^2(\mathbb{R}^2)$ stand for a stationary potential, and consider a continuity equation of the form,

$$\partial_t \rho(t,x,y) - \varepsilon \nabla \cdot \left[\exp(\frac{V}{\varepsilon})\nabla\left(\exp(-\frac{V}{\varepsilon})\rho\right)\right] = 0, \qquad x,y \in \mathbb{R}^2, \tag{5.1}$$

for which $\bar\rho(x,y) = \exp(V(x,y)/\varepsilon)$ is clearly a steady-state. Then, a simple benchmark consists in picking a random perturbation of $\bar\rho$ restricted to $\Omega = (0,1)^2$ as an initial data (with unperturbed Dirichlet boundaries) and compare the emerging numerical steady-state with the corresponding restriction of $\bar\rho$. This is especially appealing for,

$$V(x,y) = -\left(\frac{3}{2}|x'|^2 + 5|y'|^2\right), \qquad (x', y') = \mathcal{R}_\theta\left(x - \frac{1}{2}, y - \frac{1}{2}\right),$$

being $\mathcal{R}_\theta$ the usual rotation matrix of angle $\theta = \frac{\pi}{6}$ and $\varepsilon = 0.65$ because it allows to compare with both the "2D Steklov scheme" studied in [18, page 189] and usual finite-differences [7] (involving an upwind discretization). Starting from random perturbations of $\bar\rho$, pointwise relative errors are scrutinized for the three schemes,

$$e(\Delta x) := \max_{i,j}\left\{\left|\frac{\rho_{i,j}^N - \bar\rho(x_i,y_j)}{\bar\rho(x_i,y_j)}\right|, \; N\Delta t \simeq 1 \text{ the numerical steady-state}\right\},$$

Grid points	"2D Green" error	"2D Steklov" error	FD error
8×8	0.0036815	0.0096818	0.1401012
12×12	0.0018102	0.0050208	0.1149618
16×16	0.0010253	0.0030357	0.0942922
24×24	0.0004318	0.0015190	0.0706629
32×32	0.0002163	0.0009252	0.0562096
48×48	0.0000851	0.0005099	0.0402375

TABLE 5.1
Relative pointwise errors at steady-state for (4.2), the scheme in [18, §5.2] and usual FD.

on several (coarse) computational grids: see Table 5.1. Hence, it is quite clear that, for the benchmark (5.1), the "Green scheme" (4.2) is of second order in Δx. The order of accuracy of the "Steklov scheme", proposed in [18, §5.2], appears to be $\frac{3}{2}$.

5.2. Incompressible Navier-Stokes models. In $\mathbb{R}^2$, the incompressible Navier-Stokes-Coriolis system in the so-called "β-plane" approximation reads, (see [3, 10, 28])

$$\partial_t \omega + \nabla^\perp \psi \cdot \nabla \omega - \beta \partial_x \psi = \Delta \omega / Re, \qquad -\Delta \psi = \omega.$$

However, it is possible to reformulate this problem in a more convenient form:

$$\partial_t \zeta - \nabla \cdot \left(\frac{\nabla \zeta}{Re} - \zeta\, \nabla^\perp \psi\right) = f(x, y), \qquad -\Delta \psi = \zeta - \beta y, \tag{5.2}$$

being ζ the "potential vorticity", [13]. System (5.2) behaves differently depending on the domain: for periodic ones, a slow-fast decoupling occurs along with a decay onto "zonal jets" [3], but in bounded ones, currents appear on one side through a layer on the stream function [10, 28]. Usual Navier-Stokes equations are recovered with $\beta = 0$.

5.3. Classical lid-driven cavity benchmark. The most classical numerical test for any discretization of Navier-Stokes equations ($\beta = 0$) is the lid-driven cavity, for which very accurate results are to be found in [16]. The scheme (4.2) was set up to carry out this problem, the stream function ψ being deduced from the vorticity ω at each time-step by means of a standard 5-points finite-difference solver. On Fig. 5.1, the outcome of (4.2) with random initial data is shown for three cases:

- $Re = 100$, grid 35×35, no secondary vortex;
- $Re = 1000$, grid 65×65, two secondary vortices (see Fig. 5.3, left);
- $Re = 3200$, grid 95×95, three secondary vortices (see Fig. 5.3, right).

To compare with, results of a simpler dimensional-splitting Il'in/Scharfetter-Gummel (1.4)–(1.5) discretization (on a 45×45 grid) are indicated on Fig. 5.2. Comparison with reference values from [16] indicates a non-negligible deviation; worse, it seems that such a scheme isn't able to stabilize as residues begin to grow again around $t \simeq 6$. The agreement with reference values is fairly satisfying, especially for $Re = 3200$; transients are quite complex because the scheme tries, between $t = 15$ and $t = 35$, to stabilize the problem with only two secondary vortices, hence a stagnation of residues shown on Fig. 5.1, in sharp contrast with what happens for lower Reynolds numbers.

5.4. Western currents for Navier-Stokes-Coriolis. Now, we proceed with values $\beta \neq 0$ in (5.2), but we restrict ourselves to bounded domains, in which strong lateral currents are expected to materialize, in qualitative agreement with the ones in Northern Atlantic ocean, see [9, 10, 12, 28]. Two different situations will be considered:

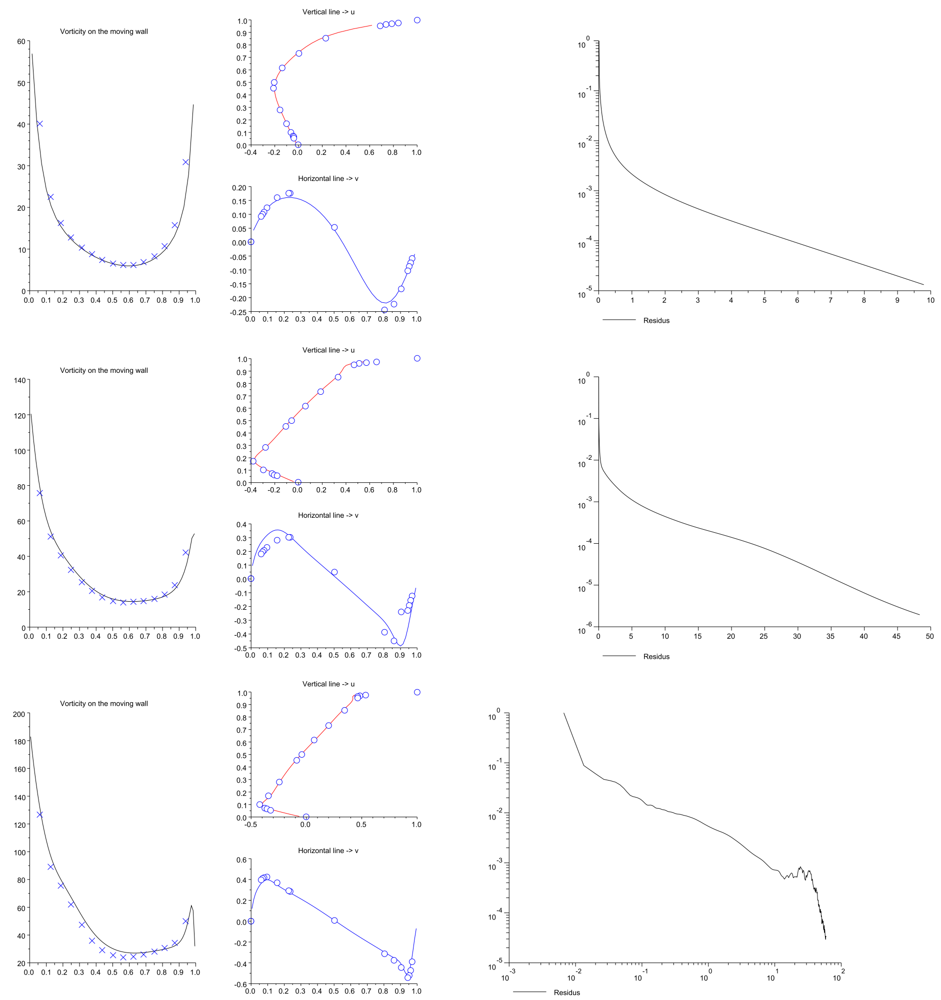

FIGURE 5.1. *Comparison with reference values [16] (left) and time-decay of residues (right).*

one with a very elementary computational domain (like in [9]), the other in a more realistic geometry (see Fig. 5.5). To cope with such a geometry while sticking to a Cartesian finite-differences framework, one strategy is to set up a "masking technique" for which both islands and continents are rendered through a given set $\Xi \in \mathbb{R}^2$. The Poisson equation in (5.2) for the stream function gets modified as follows,

$$-\Delta\psi + M\chi_\Xi(x,y)\psi = \zeta - \beta y, \qquad M \gg 1,$$

with Dirichlet boundary conditions. The function χ_Ξ is the indicator of the set Ξ and acts as a strong penalization term; such a damped Poisson equation can be efficiently handled by means of the "discrete weighted mean" schemes proposed in [15, 34] (or the stationary ones in [18]). No-slip (Thom) boundary values are prescribed on ζ on $\partial\Xi$, whereas slip conditions are imposed when $\partial\Omega$ corresponds to the ocean. Transients for both the cases are comparable, with a quick formation of currents on the left side of the domain, and an oscillating decay of energy which allows to reach a numerical

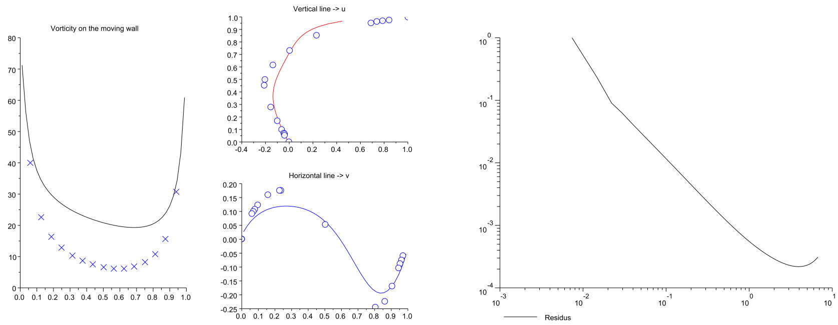

FIGURE 5.2. *Dimensional-split Il'in/Scharfetter-Gummel results with Re=100 and* 45×45 *points.*

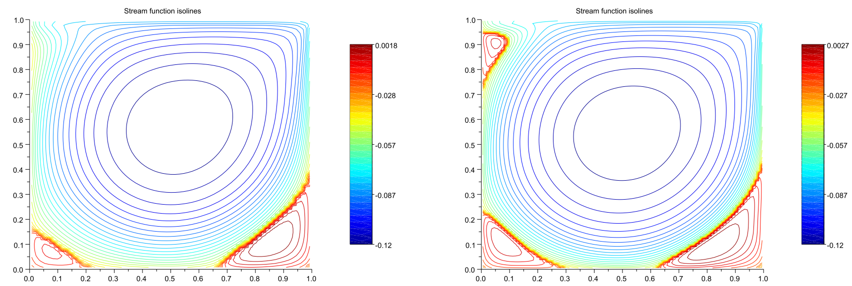

FIGURE 5.3. *Stream function: Re=1000,* 65×65 *points (left); Re=3200,* 95×95 *points (right).*

steady-state. The oscillations are clearly visible on the time-residues (Fig. 5.4, right) obtained with the simple geometry, a 50×50 grid, $f \equiv 0$, $\beta = 60$ and $Re = 200$. In the more intricate case, $\alpha = 0.3$, $Re = 400$, and the wind-forcing term is (see [9]),

$$f(x, y) = -\pi \sin(\pi(2 - x)(y + 0.15)), \qquad x, y \in \Omega := (0, 1) \times (-0.3, 0.7).$$

6. Conclusion. The construction of reliable numerical fluxes for multi-dimensional problems is a difficult task, see for instance [6, 17, 26] and references within. Accordingly, a "genuinely two-dimensional" finite-difference scheme was built for equation of the type (1.1) by taking advantage of explicit calculations which can be achieved on local Dirichlet-Green function for the convection-diffusion operator in a disk. Numerical fluxes are thus defined as its radial derivative, so that a 4-points trigonometric interpolation on each Delaunay circle allows to derive a feasible scheme on a uniform Cartesian grid. Comparable procedures based on local Green's functions were previously considered, see e.g. [4, 14, 15, 27, 30]; however, to the best of our knowledge, a full 2D computation (as done here) doesn't seem to have been achieved before. Beside, concerning incompressible fluid motion, divergence-free constraints were taken into account in [22]. Two-dimensional extensions of 1D Il'in/Scharfetter-Gummel's famous scheme were more quickly studied in the realm of Finite-Element methods (FEMs), with mixed elements [8]. Later, Galerkin and Petrov-Galerkin formulations based on tensorial products of 1D solutions were given in [23, 24, 29, 27, 33], too.

Acknowledgment. Thanks are due to both Prof. Laure Saint-Raymond, for her assistance in devising benchmarks for the β-plane Navier-Stokes model, and Prof.

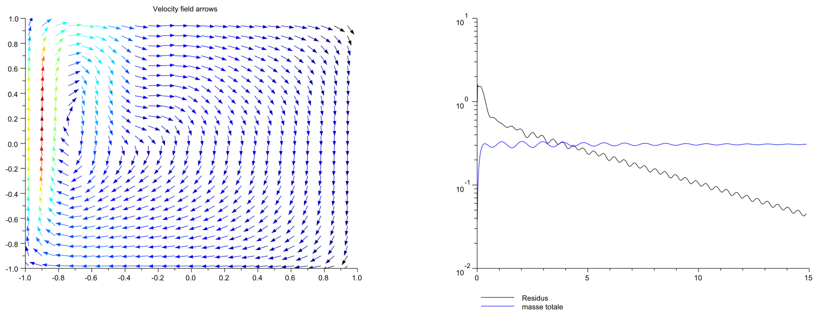

FIGURE 5.4. *Velocity field (left) and time-decay of residues (right) for $\beta = 60$ and Re=200.*

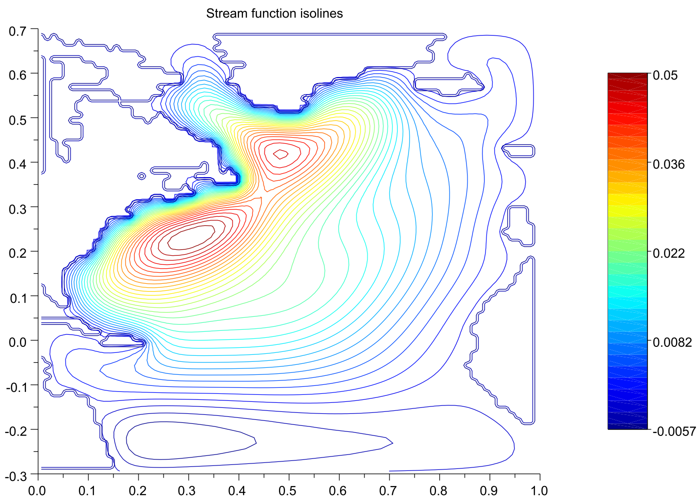

FIGURE 5.5. *Stream function in a more realistic domain, for $\beta = 60$ and Re=400.*

Kare Olaussen for his precious help in deriving Dirichlet-Green's functions.

REFERENCES

[1] M. Abramowitz, I.A. Stegun, **Handbook of Mathematical Functions**, Wiley N.Y., 1972.

[2] M. Ainsworth, W. Dorfler, *Fundamental systems of numerical schemes for linear convection-diffusion equations and their relationship to accuracy*, Computing **66** (2001) 199–229.

[3] M. Al-Jaboori, D. Wirosoetisno, *Navier-Stokes equations on the β-plane*, DCDS-B **16** (2011) 687–701.

[4] O. Axelson, E. Glishkov, N. Glishkova, *The local Green's function method in sinfularly perturbed convection-diffusion problem*, Math. Comput. **78** (2009) 153–170.

[5] I. Babuska, J.E. Osborn, *Generalized finite element methods: their performance and their relation to mixed methods*, SIAM J. Numer. Anal. **20** (1983) 510–536.

[6] F. Bouchut, Y. Jobic, R. Natalini, R. Occelli, V. Pavan, *Second-order entropy satisfying BGK-FVS schemes for incompressible Navier-Stokes equations*, preprint (2016).

[7] F. Brezzi, A. Russo, *Choosing bubbles for advection-diffusion problems*, Math. Models & Methods Applied Sci. **4** (1994) 571–587.

[8] F. Brezzi, D. Marini, P. Pietra, *Two-dimensional exponential fitting and applications to drift-diffusion models*, SIAM J. Numer. Anal. **26** (1989) 1342–1355.

[9] K. Bryan, *A numerical investigation of a nonlinear model of a wind-driven ocean*, J. Atmospheric Sci. **20** (1963) 594–606.

[10] A.-L. Dalibard; L. Saint-raymond, **Mathematical study of degenerate boundary layers: A large scale ocean circulation problem**, Memoirs of AMS (to appear).

[11] Dean R. Duffy, **Green functions and applications**, *Chapman & Hall/CRC Press* (2001) ISBN 1-58488-110-0.

[12] M. Endoh, *A numerical experiment on the variations of western boundary currents*. Part I. J. Oceanog. Soc. Japan **29** (1973) 16–27.

[13] G.J. Fix, *Finite element models for ocean circulation problems*, SIAM J. Applied Math. **29** (1975) 371–387.

[14] S. Franz, N. Kopteva, *Green's function estimates for a singularly perturbed convection-diffusion problem* J. Differential Equations, **252** (2012) 1521–1545.

[15] E.C. Gartland Jr., *Discrete weighted mean approximation of a model convection-diffusion equation*, SIAM J. Sci. Stat. Comp. **3** (1982) 460–472.

[16] U. Ghia, K.N. Ghia, C.T. Shin, *High-Re solutions for incompressible flow using the Navier-Stokes equations and a multigrid method*, J. Comput. Phys. **48** (1982) 387–411.

[17] L. Gosse, *A two-dimensional version of the Godunov scheme for convex, scalar balance laws*, SIAM J. of Numer. Anal. **52** (2014) 626–652.

[18] L. Gosse, *Viscous equations treated with $\mathcal{L}$-splines and Steklov-Poincaré operator in two dimensions*, in **Innovative Algorithms & Analysis**, DOI: 10.1007/978-3-319-49262-9_6.

[19] Houde Han, Zhongyi Huang, R. Bruce Kellogg, *A Tailored Finite Point Method for a Singular Perturbation Problem on an Unbounded Domain*, J Sci. Comput. (2008) **36**: 243–261.

[20] T. Hou, B. Wetton, *Second-order convergence of a projection scheme for the incompressible Navier-Stokes with boundaries*, SIAM J. Numer. Anal. **30** (1993) 609–629.

[21] A.M. Ilin, *A difference scheme for a differential equation with a small parameter affecting the highest derivative*, in Russian, Matematicheskie Zametki **6** (1969) 237–248.

[22] L.R.M. Maas, *A closed form Green function describing diffusion in a strained flow field*, SIAM J. Applied Math. **49** (1989) 1359–1373.

[23] E. O'Riordan, M. Stynes, *A uniformly accurate finite element method for a singularly perturbation problem in conservative form*, SIAM J. Numer. Anal. **23** (1986) 369–375.

[24] E. O'Riordan, M. Stynes, *A globally uniformly convergent finite element method for a singularly perturbed elliptic problem in two dimensions*, Math. Comput. **57** (1991) 47–62.

[25] H.-G. Roos, *Ten ways to generate the Il'in and related schemes*, J. Comput. Applied Math. **53** (1993) 43–59.

[26] P.L.Roe, D.Sidilkover, *Optimum positive linear schemes for advection in 2 and 3 dimensions*, SIAM J. Numer. Anal. **29** 1542–1568, 1992.

[27] H.-G. Roos, M. Stynes, L. Tobiska, **Robust numerical methods for singularly perturbed differential equations. Convection-diffusion-reaction and flow problems**; 2nd edition. Springer Series in Comput. Math. **24** (2008). ISBN: 978-3-540-34466-7.

[28] L. St-Raymond, *The role of boundary layers in large-scale ocean circulation*, in **Mathematical Models and Methods for Planet Earth**, Springer INdAM Series **6** (2014) 11–24.

[29] R. Sacco, M. Stynes, *Finite Element Methods for Convection-Diffusion Problems Using Exponential Splines on Triangles*, Computers Math. Applic. **35** (1998) 35-45.

[30] Alexander A. Samarskii, **The Theory of Difference Schemes**, *Chapman & Hall/CRC Press* (2001) ISBN 9780824704681.

[31] H. L. Scharfetter and H. K. Gummel, *Large signal analysis of a silicon Read diode oscillator*, IEEE Trans. Electron Devices **16** (1969) 64–77.

[32] L.L. Schumaker, **Spline functions: basic theory**, Third edition. Cambridge University Press, Cambridge (2007). ISBN: 978-0-521-70512-7

[33] Yintzer Shih, Jun-Yong Cheng, Kuen-Tsann Chen, *An exponential-fitting finite element method for convection-diffusion problems*, Applied Math. Comput. **217** (2011) 5798–5809.

[34] J.B.R. do Val, M.G. Andrade, On mean value solutions for the Helmholtz equation on square grids, Applied Numer. Math. **41** (2002) 459–479.